Available online at www.sciencedirect.com
SCIENCE DIRECT®
Computers and Chemical Engineering 28 (2004) 2037–2052
Computers & Chemical Engineering
www.elsevier.com/locate/compchemeng

An MPEC formulation for dynamic optimization of distillation operations

Arvind U. Raghunathan [a], M. Soledad Diaz [b], Lorenz T. Biegler [a,*]

[a] *Department of Chemical Engineering, Carnegie Mellon University, Pittsburgh, PA 15213, USA*
[b] *Planta Piloto de Ingenieria Quimica, PLAPIQUI (UNS-CONICET), Bahia Blanca, Argentina*

Received 10 October 2003; received in revised form 26 March 2004; accepted 26 March 2004

Available online 18 May 2004

Abstract

We consider the dynamic optimization of chemical processes with changes in the number of equilibrium phases. Recent work has shown that transitions in the number of phases can be modeled as a mathematical program with equilibrium constraints (MPEC). This study generalizes the MPEC to consider dynamic characteristics. In particular, we describe a simultaneous discretization and solution strategy for dynamic optimization problems with complementarity constraints. These discretized problems are then solved with IPOPT-C, a recently developed barrier method for MPEC problems. Our approach is applied to two distillation examples. In the first, we consider the optimal startup of a binary batch distillation problem. In the second, we consider the dynamic operation of a cryogenic column for the separation of natural gas liquids. Both cases demonstrate the effectiveness of the approach on large scale MPEC problems.

Keywords: Dynamic optimization; Nonlinear programming; Barrier methods; Complementarity conditions; Distillation

1. Introduction

Recent developments in numerical solvers and modeling platforms have led to widespread interest in the simulation and optimization of dynamic process models. Along with the optimization of dynamic models in process engineering, it becomes important to consider the modeling of discrete events in many dynamic simulation and optimization problems. In chemical processes, examples of these phenomena include phase changes in vapor–liquid equilibrium systems, changes in modes in the operation of safety and relief valves, vessels running dry or overflowing, discrete decisions made by control systems and explosions due to accidents. These actions can be reversible or irreversible with the state profiles and should be modeled with appropriate logical constraints. An interesting presentation on modeling discrete events can be found in Barton, Allgor, Feehery, and Galan (1998). The simulation of these events is often triggered by an appropriate discontinuity function which monitors a change in the condition and leads to a change in the state equations. These changes can be reformulated either as binary decision variables (Barton & Park, 1997) or by using complementarity conditions (with non-negative continuous variables x and y alternately set to zero). These additional variables can then be embedded within optimization problems.

The incorporation of discrete decisions using either binary or integer variables leads to mixed integer optimization problems. Here, several studies have considered the solution of Mixed Integer Dynamic Optimization (MIDO) problems. In particular, Avraam, Shah, and Pantelides (1998) developed a complete discretization of the state and control variables to form a mixed integer nonlinear program. On the other hand, Allgor and Barton (1999) apply a sequential strategy and discretize only the control profile. In this case, careful attention is paid to the calculation of sensitivity information across discrete decisions that are triggered in time.

In contrast to mixed integer formulations, many discrete decisions can be modeled through complementarity relations. These include recent work in modeling dynamic hybrid systems (Heemels, DeSchutter, & Bemporad, 2001; van der Schaft & Schumacher, 1998), as well as the use of complementarity to model disjunctions (Stein, Oldenburg, & Marquardt, 2004). Introducing complementarity relations leads to a nonlinear programming formulation without integer variables. Stein et al. (2004) also propose alternative formulations for modeling discrete decisions using comple-

* Corresponding author. Tel.: +1-412-268-2232; fax: +1-412-268-7139.
E-mail address: biegler@cmu.edu (L.T. Biegler).

0098-1354/$ – see front matter © 2004 Published by Elsevier Ltd.
doi:10.1016/j.compchemeng.2004.03.015

mentarities. Nevertheless, the introduction of complementarity conditions does introduce additional nonconvexity into the problem, which would not be observed, for instance, in the NLP subproblems of a mixed integer programming approach.

In leading to a nonlinear programming framework, complementarity conditions can be handled naturally through application of barrier methods (Raghunathan & Biegler, 2003). This class of problems can also be generalized to Mathematical Programs with Equilibrium Constraints (MPECs). MPECs represent an exciting new field in mathematical programming. While applications of MPECs have long been recognized in game theory, transportation planning, economics and engineering design, little work has been done in developing efficient algorithms for their solution. A broad survey of these applications can be found in (Harker & Pang, 1990; Luo, Pang, & Ralph, 1996). In process engineering, these problems stem from bilevel and multilevel optimization problems (Clark & Westerberg, 1990; Floudas & Grossmann, 1987; Sahin & Ciric, 1998) as well as optimization of hybrid (discrete and continuous) systems (Stein et al., 2004). Included in this class are optimization problems with phase equilibrium constraints, as in equilibrium stage processes (Raghunathan & Biegler, 2003), and cellular models based on metabolic pathways (Raghunathan, Perez-Correa, & Biegler, 2003).

In this work, we consider the optimization of differential algebraic systems with complementarity constraints. The complementarity constraints posed here model discontinuous system behavior such as appearance of phases and liquid overflows. The dynamic problem is discretized in time using collocation on finite elements to yield an MPEC. To solve the MPEC we apply a primal-dual interior point approach. The interior point approach (Raghunathan & Biegler, 2003) is particularly useful in the context of large-scale inequality constrained optimization that often results from a spatial or temporal discretization (Wächter, 2002). In particular, we have incorporated the MPEC formulation into the IPOPT code (Wächter, 2002; Wächter & Biegler, 2004) along with algorithmic modifications to treat the complementarity constraints more efficiently. This code (called IPOPT-C) has been interfaced to the AMPL modeling system and has been tested on a set of library MPEC problems (Leyffer & Fletcher, 2000). Preliminary results (Raghunathan & Biegler, 2003) show that this implementation compares well against competing barrier algorithms. In previous work, we have tested this approach on a number of steady state process optimization problems with phase equilibrium constraints. These include distillation optimization problems with disappearing vapor and liquid phases on equilibrium stages. Preliminary results (Raghunathan & Biegler, 2003) show that this approach leads to better and more uniform performance than the smoothing approach used in our previous studies (Gopal & Biegler, 1999; Lang & Biegler, 2001). We demonstrate the effectiveness of our approach on two challenging distillation operations. The results presented here are the most extensive dynamic optimization applications of nonlinear programming algorithms with MPEC's.

The next section provides the general problem statement for MPECs that occur in dynamic systems as well as our solution strategy for solving these problems. In Section 3, we outline dynamic optimization problems with complementarity for the distillation cases that we consider. In addition to a general model that includes vapor holdup we describe a simplification with only liquid holdup. In Sections 5 and 6, we consider two cases, a batch distillation and a cryogenic column, respectively. In both cases, the optimal profiles contain transitions with changes in the number of phases on all of the trays. Concluding remarks are then given in Section 7.

2. Dynamic optimization with complementarity

The general DAE optimization problem can be stated as follows:

$$\min_{z_d(t), z_a(t), u(t), t_f, p} \varphi(z_d(t_f), z_a(t_f), u(t_f), t_f, p) \tag{1}$$

s.t. Semi-explicit DAE model:

$$\frac{\mathrm{d}z_d(t)}{\mathrm{d}t} = F(z_d(t), z_a(t), u(t), t, p) \tag{2}$$

$$0 = G(z_d(t), z_a(t), u(t), t, p) \tag{3}$$

$$0 \le z_{a_1}(t) \perp z_{a_2} \ge 0 \tag{4}$$

Initial conditions:

$$z_d(0) = z_d^0 \tag{5}$$

Point conditions:

$$H_s(z_d(t_s), z_a(t_s), u(t_s), t_s, p) = 0 \quad \text{for } s \in \{1, \ldots, n_S\} \tag{6}$$

Bounds:

$$\begin{aligned} z_d^L &\le z_d(t) \le z_d^U \\ z_a^L &\le z_a(t) \le z_a^U \\ u^L &\le u(t) \le u^U \\ p^L &\le p \le p^U \\ t_f^L &\le t_f \le t_f^U \end{aligned} \tag{7}$$

where φ is the scalar objective function, F the right hand sides of differential equation constraints, G the algebraic equation constraints, H_s the additional point conditions at fixed times t_s, z_d the differential state profile vectors, z_d^0 the initial values of differential state profile vector z_d, *assumed consistent*, z_a the algebraic state profile vectors, z_{a_j} the subvector of algebraic state profiles with $j = 1, 2$, u the control profile vectors, p the time-independent parameter vector, and t_f is the final time.

Note that bounds on the state variables allow us to handle path constraints without loss of generality. Included among

the algebraic constraints are complementarity conditions (4) between z_{a_1} and z_{a_2} subvectors of the vector of algebraic variables, z_a for all time t. We use the "$\perp$" notation to define complementarity between the arguments, i.e.,

$$z_{a_1}^{(i)}(t), z_{a_2}^{(i)}(t) \geq 0 \quad z_{a_1}^{(i)}(t) z_{a_2}^{(i)}(t) = 0 \tag{8}$$

for each of the components i of the subvectors and all time t. In the above $z_{a_1}^{(i)}$ refers to the ith component of z_{a_1}. Finally we assume that for specified values of $z_d(t)$, $u(t)$ and p, the algebraic equations and complementarity constraints can always be solved for the the algebraic variables, $z_a(t)$. This is analogous to the *index 1* property for the DAE.

This DAE optimization problem is converted to algebraic form by approximating state and control profiles by a family of polynomials on finite elements ($t_0 < t_1 < \cdots < t_{ne} = t_f$). Here, we use a monomial basis representation (Bader & Ascher, 1987) for the differential profiles, as follows:

$$z_d(t) = z_{d,i-1} + h_i \sum_{q=1}^{\text{ncol}} \Omega_q \left(\frac{t - t_{i-1}}{h_i} \right) \left(\frac{\mathrm{d}z_d}{\mathrm{d}t} \right)_{i,q} \qquad t_{i-1} \leq t \leq t_i \tag{9}$$

where $z_{d,i-1}$ is the value of the differential variable at the beginning of element i, h_i the length of element i, $(\mathrm{d}z_d/\mathrm{d}t)_{i,q}$ is the value of its first derivative in element i at the collocation point q, and Ω_q is the polynomial of order ncol, satisfying

$$\Omega_q(0) = 0 \qquad \text{for } q = 1, \ldots, \text{ncol}$$
$$\Omega_q'(\rho_r) = \delta_{q,r} \qquad \text{for } q, r = 1, \ldots, \text{ncol}$$

where $\delta_{q,r}$ is the Kronecker delta and ρ_r is the location of the rth collocation point within each element. Continuity of the differential profiles is enforced by

$$z_{d,i} = z_{d,i-1} + h_i \sum_{q=1}^{\text{ncol}} \Omega_q \left(\frac{t_i - t_{i-1}}{h_i} \right) \left(\frac{\mathrm{d}z_d}{\mathrm{d}t} \right)_{i,q}. \tag{10}$$

Here, Radau collocation points are used because they allow us to set constraints easily at the end of each element and they stabilize the system more efficiently if high index DAEs are present. In addition, the control and algebraic profiles are approximated using a similar monomial basis representation which takes the form:

$$z_a(t) = \sum_{q=1}^{\text{ncol}} \psi_q \left(\frac{t - t_{i-1}}{h_i} \right) z_{a,i,q} \tag{11}$$

$$u(t) = \sum_{q=1}^{\text{ncol}} \psi_q \left(\frac{t - t_{i-1}}{h_i} \right) u_{i,q}. \tag{12}$$

Here $z_{a,i,q}$ and $u_{i,q}$ represent the values of the algebraic and control variables, respectively, in element i at collocation point q. ψ_q is the Lagrange polynomial of order ncol satisfying

$$\psi_q(\rho_r) = \delta_{q,r} \quad \text{for } q, r = 1, \ldots, \text{ncol}.$$

From (10), the differential variables are required to be continuous over time, while the control and algebraic variables are allowed to have discontinuities at the boundaries of the elements. It should be mentioned that with representation (10), the bounds on the differential variables are enforced directly at element boundaries; however, they can be enforced at all collocation points by writing appropriate point constraints (6).

For this study, we assume that the number of finite elements, *ne*, and their lengths are pre-determined. Substitution of Eqs. (9)–(12) into (1)–(7) leads to the MPEC problem given by:

$$\min_{x \in \mathbb{R}^n, w \in \mathbb{R}^m, y \in \mathbb{R}^m} \quad f(x, w, y) \tag{13}$$

$$\text{s.t.} \quad c(x, w, y) = 0, \quad x, w, y \geq 0 \tag{14}$$

$$w^{(i)} y^{(i)} = 0, \quad i = 1, \ldots, m \tag{15}$$

where we now consider an augmented set of variables (x, w, y) and $w^{(i)}$ refers to ith component of w. For simplicity of presentation, we assume only simple bounds on the variables. General inequality constraints can be easily converted to the above form by addition of slack variables. In the above formulation, we identify w, y with the discretization of z_{a_1}, z_{a_2} respectively. The discretization of the differential variable z_d, algebraic variables z_a with the exception of z_{a_1}, z_{a_2}, the controls u and the parameter vector p constitute the vector x. Note that the addition of complementarity conditions (15) leads to a violation of convergence assumptions for most nonlinear programming algorithms (e.g., linear independence of the constraint gradients) and can cause these algorithms to fail. Anitescu (2001) and Fletcher, Leyffer, Ralph, and Scholtes (2002) have shown theoretical evidence for good local convergence behavior of *active set* NLP algorithms on MPECs. Sequential Quadratic Programming (SQP) algorithms such as filter-SQP (Fletcher, Gould, Leyffer, Toint, & Wächter, 1999) and SNOPT (Gill, Murray, & Saunders, 2002) are some examples of *active set* algorithms that exhibit favorable convergence behavior on MPECs. However, active set algorithms are prone to inefficiencies on large-scale inequality constrained problems. This is largely due to the combinatorially intensive subproblem that arises when identifying the *active* constraints at the solution. Instead, recent work on interior point algorithms for NLPs has shown that they greatly reduce this deficiency, paving the way for efficient solution of large-scale nonlinear programming problems. The effectiveness of interior point methods has been demonstrated on a number of process engineering problems (Cervantes & Biegler, 1998; Cervantes, Wächter, Tütüncü, & Biegler, 2000; Wächter, 2002). This has been our motivation in looking to an interior point algorithm for solving MPECs. More recently, a large scale interior point algorithm, IPOPT (Wächter, 2002; Wächter & Biegler, 2004) has been developed with proven convergence behavior (Wächter & Biegler, 2004) and favorable practical performance (Wächter, 2002) on a large

class of problems. In the remainder of the subsection we present an extension of interior point methods for handling complementarity constraints and also discuss the issue of incorporating this extension within an NLP interior point algorithm such as IPOPT.

2.1. NLP interior point method

A naive application of the NLP interior point algorithm reformulates the MPEC problem (15) by replacing the bound constraints with logarithmic barrier terms as,

$$\begin{aligned} \min_{x\in\mathbb{R}^n, w\in\mathbb{R}^m, y\in\mathbb{R}^m} \quad & f(x,w,y) \\ -\mu & \left(\sum_{i=1}^{n}\ln(x^{(i)}) + \sum_{i=1}^{m}\ln(w^{(i)}) + \sum_{i=1}^{m}\ln(y^{(i)})\right) \\ \text{s.t.} \quad & c(x,w,y) = 0 \\ & Wy = 0 \end{aligned} \tag{16}$$

where $\mu > 0$ is the barrier parameter and $W := \mathrm{diag}(w^{(1)}, \ldots, w^{(m)})$ is $m \times m$ diagonal matrix with components of y on the diagonal. The algorithm is initialized with $\mu > 0$ and solved to a tolerance that is proportional to μ. Subsequently, the barrier parameter μ is reduced and a sequence of problems is solved for decreasing values of μ. The limit of the solutions as $\mu \to 0$ can be shown to be the solution to the original problem under reasonable assumptions. For a positive value of the barrier parameter, none of the variables can lie at their bound as this will result in an unbounded objective value. Hence, solutions lying at a bound can only be obtained in the limit ($\mu \to 0$). Refer to Fiacco and McCormick (1968) and Forsgren, Gill, and Wright (2002) for existence of barrier solutions and convergence of barrier solutions to a solution of the NLP. Unfortunately, the complementarity constraints in the above barrier problem (16) requires at least one of $w^{(i)}$ and $y^{(i)}$ to vanish, and results in a problem that has no interior feasible points. This might be considered as a limitation in using a NLP barrier algorithm for the solution of MPECS which require the existence of a strictly feasible interior. In the following we describe a modification to the barrier problem that avoids this limitation.

2.2. Relaxed barrier problem

The interior point method for NLPs has a straightforward extension to solving MPEC problems. The complementarity constraint,

$$w^{(i)}y^{(i)} = 0 \quad \text{is relaxed as} \quad w^{(i)}y^{(i)} \le \delta\mu$$

where $\delta > 0$ renders the problem strictly feasible. Note that μ is the same as the barrier parameter. The interior point algorithm will drive the barrier parameter μ to zero as part of the solution process and hence, the complementarity constraints are recovered in the limit. The strength of the relaxation lies in our ability to provide a fast local convergence guarantee to a smooth solution of the MPEC. A brief summary of the properties of the algorithm applied to the relaxed problem will be provided in the following. We can restate the barrier problem by addition of non-negative slack variables, $s \in \mathbb{R}^m$ for the inequality relaxation of the complementarity constraints and appending the logarithmic barrier term to the objective as follows:

$$\begin{aligned} \min_{x\in\mathbb{R}^n, w\in\mathbb{R}^m, y\in\mathbb{R}^m, s\in\mathbb{R}^m} \quad & f(x,w,y) \\ -\mu & \left(\textstyle\sum_{i=1}^{n}\ln(x^{(i)}) + \sum_{i=1}^{m}\ln(w^{(i)}) + \sum_{i=1}^{m}\ln(y^{(i)})\right) \\ -\mu & \textstyle\sum_{i=1}^{m}\ln(s^{(i)}) \\ \text{s.t.} \quad & c(x,w,y) = 0 \\ & Wy + s = \delta\mu. \end{aligned} \tag{17}$$

Introducing multipliers for variable bounds leads to the following optimality conditions of (17):

$$\begin{aligned} &\nabla_x f(x,w,y) + \nabla_x c(x,w,y)\lambda_c - \lambda_x = 0 \\ &\nabla_w f(x,w,y) + \nabla_w c(x,w,y)\lambda_c + Y\lambda_{cc} - \lambda_w = 0 \\ &\nabla_y f(x,w,y) + \nabla_y c(x,w,y)\lambda_c + W\lambda_{cc} - \lambda_y = 0 \\ &X\lambda_x - \mu e_n = 0 \\ &W\lambda_w - \mu e_m = 0 \\ &Y\lambda_y - \mu e_m = 0 \\ &S\lambda_{cc} - \mu e_m = 0 \\ &c(x) = 0 \\ &Wy + s - \delta\mu = 0 \end{aligned} \tag{18}$$

where e_n is a vector of all ones of dimension n, λ_x, λ_w, λ_y, λ_{cc} are the multipliers for the nonnegativity bounds on variables x, w, y, s respectively and λ_c are multipliers for the constraint c. The above approach of relaxing the complementarity constraints can be easily incorporated within most interior point algorithms with minimal modifications. The proposed framework for solving MPECs has been incorporated within such an NLP interior point algorithm, IPOPT.

2.3. IPOPT-C—extension to IPOPT for solving MPECs

IPOPT (Wächter, 2002; Wächter & Biegler, 2004) is a large-scale interior point algorithm for solving NLPs. The algorithm solves the problem (17) approximately for a fixed barrier parameter, μ and then reduces it successively. IPOPT applies Newton's method to the optimality conditions of the barrier problems (18) to determine a search direction which will yield the next iterate. The step size is first reduced so that the resulting iterate satisfies the bounds on the variables. However, this is not sufficient to ensure global convergence of the algorithm for iterates far removed from a solution. A filter line search method is employed to obtain an iterate that has sufficiently decreased the objective value or the constraint infeasibility. More details on the algorithm and convergence can be obtained from Wächter and Biegler (2004) and the thesis of Wächter (2002).

This interior point algorithm has been interfaced to AMPL (Fourer, Gay, & Kernighan, 2001) which provides the algorithm with exact derivative (first and second) information and can also easily communicate complementarity between variables through the *complements* operator. The interface to AMPL has been extended to take advantage of the operator and parse the relaxed complementarity constraint to IPOPT. We refer to IPOPT with the extended features to handle complementarity constraints as IPOPT-C. The step calculation in IPOPT-C differs from IPOPT in that the Jacobian of the optimality conditions (18) is modified so that the system is nonsingular, even in the limit as the barrier parameter is driven to zero, $\mu \to 0$. This is necessary to show that the algorithm solves a well-posed set of equations at every iteration. Further, the modification is made proportional to the error in the optimality conditions at the current iterate. This ensures that the modification decreases as we approach a solution of the MPEC. IPOPT-C has been shown to be superlinearly convergent (Raghunathan & Biegler, 2004) to a solution of the MPEC. Encouraging practical performance on a large class of MPEC test problems is also reported in the same paper.

3. Distillation models

We now consider two dynamic distillation models used in our later MPEC case studies. The two models are index one and index two, respectively, and the second considers the common simplification of neglecting vapor holdup. In both cases, we apply a generalization of the complementarity conditions used for phase equilibrium that is described in (Raghunathan & Biegler, 2003).

For these models we assume potential feeds on all of the trays and adopt the following set notation. The number of trays in the column is assumed to be N inclusive of both the reboiler and condenser, with trays numbered from the bottom. The set TRAYS $:= \{1, \ldots, N\}$ will denote the numbered trays and index, i subscripted to a quantity refers to that quantity associated with tray, i. The set COMP denotes the components in the column. The superscripts l and v refer to the quantities associated with the liquid and vapor phases, respectively.

The model equations are:

Total Mass balance on each tray

$$\begin{aligned}
&\frac{\mathrm{d}M_1}{\mathrm{d}t} = L_2 - V_1 - L_1 + F_1 \\
&\frac{\mathrm{d}M_i}{\mathrm{d}t} = V_{i-1} + L_{i+1} - V_i - L_i + F_i \qquad i \in \text{TRAYS} \setminus \{1, N\} \\
&\frac{\mathrm{d}M_N}{\mathrm{d}t} = V_{N-1} - V_N - D - L_N + F_N \\
&M_i(0) = M_i^0 \quad i \in \text{TRAYS}
\end{aligned} \tag{19}$$

where M_i, L_i, V_i, F_i are the holdup, liquid flowrate, vapor flowrate and feed rate on the ith tray, respectively.

Component balance on each tray

For each component $j \in$ COMP, we have:

$$\begin{aligned}
&\frac{\mathrm{d}M_{1,j}}{\mathrm{d}t} = L_2 x_{2,j} - V_1 y_{1,j} - L_1 x_{1,j} + F_1 z_{1,j}^f \\
&\frac{\mathrm{d}M_{i,j}}{\mathrm{d}t} = V_{i-1} y_{i-1,j} + L_{i+1} x_{i+1,j} - V_i y_{i,j} - L_i x_{i,j} \\
&\qquad\qquad + F_i z_{i,j}^f \quad i \in \text{TRAYS} \setminus \{1, N\} \\
&\frac{\mathrm{d}M_{N,j}}{\mathrm{d}t} = V_{N-1} y_{N-1,j} - V_N y_{N,j} - D x_{N,j} - L_N x_{N,j} \\
&\qquad\qquad + F_N z_{N,j}^f \\
&M_{i,j}(0) = M_{i,j}^0 \quad i \in \text{TRAYS}
\end{aligned} \tag{20}$$

where $M_{i,j}$, $z_{i,j}^f$, $x_{i,j}$, $y_{i,j}$ represent the hold-up, feed, liquid and vapor composition of component j on the ith tray, respectively.

Energy balance on each tray

In the following $U_i(x_i, y_i, T_i)$, $h_i^l(x_i, T_i)$ and $h_i^v(y_i, T_i)$ define the tray holdup internal energy and the specific heat content of liquid and vapor emanating from tray i. These are functions of composition of the mixture and tray temperature. For brevity we will avoid stating the arguments of U_i, h_i^l and h_i^v.

$$\begin{aligned}
&\frac{\mathrm{d}U_1}{\mathrm{d}t} = L_2 h_2^l - V_1 h_1^v - L_1 h_1^l + F_1 h_1^f + Q_r \\
&\frac{\mathrm{d}U_i}{\mathrm{d}t} = V_{i-1} h_{i-1}^v + L_{i+1} h_{i+1}^l - V_i h_i^v - L_i h_i^l + F_i h_i^f \\
&\qquad\qquad i \in \text{TRAYS} \setminus \{1, N\} \\
&\frac{\mathrm{d}U_N}{\mathrm{d}t} = V_{N-1} h_{N-1}^v - V_N h_N^v - D h_N^l - L_N h_N^l \\
&\qquad\qquad + F_N h_N^f - Q_c \\
&U_i(0) = U_i^0 \quad i \in \text{TRAYS}
\end{aligned} \tag{21}$$

with h_i^f representing the specific enthalpy of the feed stream to tray i and Q_r and Q_c are the reboiler and condenser heat loads.

Thermodynamic equations governing equilibrium

For each tray $i \in$ TRAYS

$$\begin{aligned}
&y_{i,j} = \beta_i K_{i,j}(T_i, P_i, x_i) x_{i,j} \quad j \in \text{COMP} \\
&0 = \sum_{j \in \text{COMP}} y_{i,j} - \sum_{j \in \text{COMP}} x_{i,j} \\
&\beta_i = 1 - \nu_i^l + \nu_i^v \\
&0 \le M_i^l \perp \nu_i^l \ge 0 \\
&0 \le M_i^v \perp \nu_i^v \ge 0
\end{aligned} \tag{22}$$

From (22), note that the complementarity constraints imply the following

$$\begin{aligned} &M_i^l, M_i^v > 0, && \text{then } \beta_i = 1 \\ &M_i^l = 0 < M_i^v, && \text{then } \beta_i \le 1 \\ &M_i^l > 0 = M_i^v, && \text{then } \beta_i \ge 1. \end{aligned} \tag{23}$$

Thus, the equilibrium relation is enforced only when liquid and vapor are present on a tray and relaxed otherwise. Gopal and Biegler (1999) derive the above conditions (22) as the reformulation of Gibbs free energy minimization on each tray, i which is the thermodynamic condition for the existence of a phase.

Density, holdup, pressure defining equations

For each tray $i \in$ TRAYS

$$\begin{aligned} \rho_i^l &= \frac{1}{\sum_{j\in\text{COMP}} x_{i,j}\bar{\rho}_j} \\ \rho_i^v &= \frac{P_i}{R_{\text{gas}}T_i} \\ V_i^{\text{vol}} &= \pi\left(\frac{d}{2}\right)^2 H_{\text{plate}} - \frac{M_i^l}{\rho_i^l} \\ M_i^v &= \rho_i^v V_i^{\text{vol}} \\ M_i &= M_i^v + M_i^l \\ U_i &= M_i^v(h_i^v - p_i\mathcal{V}_i^v) + M^l(h_i^l - p_i\mathcal{V}_i^l) \\ &\approx M_i^v(h_i^v - R_{\text{gas}}T_i) + M^l h_i^l \end{aligned} \tag{24}$$

where R_{gas} is the ideal gas constant, V_i^{vol} denotes the volume of vapor on each tray, $\mathcal{V}_i^l$ and $\mathcal{V}_i^v$ are the specific molar volumes for the liquid and vapor, respectively, d is the diameter of the plate, H_{plate} is the height of the plate and $\bar{\rho}_j$ is the liquid density of component j at some reference temperature. These data are taken from (Pedersen, Fredenslund, & Thomassen, 1989).

Liquid and Vapor flow definitions

All trays are modeled so that the liquid flow from a tray occurs only when there is a certain amount of liquid holdup. The liquid flowrate from trays can be stated as,

$$L_i = \begin{cases} 0, & \text{if } M_i^l \le M_{\min,i} \\ k_d(M_i^l - M_{\min,i})^{1.5}, & \text{otherwise} \end{cases} \qquad i \in \text{TRAYS} \setminus \{1\}$$

where $k_d > 0$ is a constant and $M_{\min,i}$ is the minimum holdup required on each tray in order to have a liquid flow from the tray. This condition can be modeled using complementarity conditions as,

$$\begin{aligned} &M_i^l - M_{\min,i} = M_i^{l,+} - M_i^{l,-} \\ &L_i = k_d(M_i^{l,+})^{1.5} \\ &M_i^{l,+}M_i^{l,-} = 0 \\ &M_i^{l,+}, M_i^{l,-} \ge 0 \end{aligned} \tag{25}$$

for all $i \in$ TRAYS $\setminus \{1\}$. The non-negative variables $M_i^{l,+}, M_i^{l,-}$ represent respectively the amount of liquid holdup above and below the threshold for liquid flow. The complementarity condition ensures that no more than one of $M_i^{l,+}, M_i^{l,-}$ assume a non-zero value. The vapor flow on the trays can then be defined as,

$$\begin{aligned} H_{o,i}^l &= \alpha_{\text{head}}^l \frac{M_i}{\pi(D/2)^2\rho_i^l} \quad i \in \text{TRAYS} \\ H_{o,i}^v &= \alpha_{\text{head}}^v(P_{i-1} - P_i) - H_{o,i}^l \quad i \in \text{TRAYS} \setminus \{N\} \\ H_{o,N}^v &= \alpha_{\text{head}}^v(P_N - P_{\text{out}}) \\ V_i &= \alpha_{\text{weir}}^v(H_{o,i}^v)^{0.5} \quad i \in \text{TRAYS} \end{aligned} \tag{26}$$

where $\alpha_{\text{head}}^l, \alpha_{\text{head}}^v$ are constants for defining the liquid and vapor heads, α_{weir}^v is a constant in defining the vapor flow and P_{out} is the top pressure controlling the withdrawal of the vapors from tray N.

4. Simplified model equations

The above equations assume vapor holdup. Since this quantity is typically much smaller than the total holdup, we can simplify the model considerably by eliminating variation of pressure on each tray and considering the tray holdup to be only for the liquid phase. This formulation has the advantage that the density, holdup, pressure defining equations can be eliminated and the total mass balance Eq. (19) remain the same. The remaining equations are now written as:

Component balance on each tray

For each component $j \in$ COMP, we have:

$$\begin{aligned} M_1\frac{\mathrm{d}x_{1,j}}{\mathrm{d}t} &= L_2(x_{2,j} - x_{1,j}) - V_1(y_{1,j} - x_{1,j}) \\ &\quad + F_1(z_{1,j}^f - x_{1,j}) \\ M_i\frac{\mathrm{d}x_{i,j}}{\mathrm{d}t} &= V_{i-1}(y_{i-1,j} - x_{i,j}) \\ &\quad + L_{i+1}(x_{i+1,j} - x_{i,j}) - V_i(y_{i,j} - x_{i,j}) \\ &\quad + F_i(z_{i,j}^f - x_{i,j}) \quad i \in \text{TRAYS} \setminus \{1, N\} \\ M_N\frac{\mathrm{d}x_{N,j}}{\mathrm{d}t} &= V_{N-1}(y_{N-1,j} - x_{N,j}) - V_N(y_{N,j} - x_{N,j}) \\ &\quad + F_N(z_N^f - x_{N,j}) \end{aligned} \tag{27}$$

Energy balance on each tray

$$\begin{aligned}
M_1\frac{\mathrm{d}h_1^l}{\mathrm{d}t} &= L_2(h_2^l - h_1^l) - V_1(h_1^v - h_1^l) \\
&\quad + F_1(h_1^f - h_1^l) + Q_r \\
M_i\frac{\mathrm{d}h_i^l}{\mathrm{d}t} &= V_{i+1}(h_{i+1}^v - h_i^l) \\
&\quad + L_{i-1}(h_{i-1}^l - h_i^l) - V_i(h_i^v - h_i^l) \\
&\quad + F_i(h_i^f - h_i^l) \quad i \in \text{TRAYS} \setminus \{1, N\} \\
M_N\frac{\mathrm{d}h_N^l}{\mathrm{d}t} &= V_{N-1}(h_{N-1}^v - h_N^l) - V_N(h_N^v - h_N^l) \\
&\quad + F_N(h_N^f - h_N^l) - Q_c
\end{aligned} \tag{28}$$

The thermodynamic equations are the same as in (22) except that there is no need to subscript the pressure variable with the tray index. Also, for the liquid overflow we use the same relations (25) as before. However, since we neglect the vapor holdup, calculation of the vapor flow is a little more difficult. Here the DAEs form an index 2 system with differential variables M_i, $x_{i,j}$ and h_i^l. The remaining algebraic variables need to be solved by the algebraic equations. From the above system, we see that the vapor flowrate V_i cannot be solved by this system. As a result, a reformulation to an index one system is required.

For this reformulation we differentiate the summation equation with respect to time and recover the relation:

$$\frac{\mathrm{d}}{\mathrm{d}t}\left[\sum_{j\in\text{COMP}} y_{i,j} - \sum_{j\in\text{COMP}} x_{i,j}\right] = 0$$

or equivalently (22):

$$\begin{aligned}
\sum_{j\in\text{COMP}}\Bigg[&\frac{\mathrm{d}\beta_i}{\mathrm{d}t}K_{i,j}x_{i,j} + \beta_i\frac{\partial(K_{i,j})}{\partial T_i}\frac{\mathrm{d}T_i}{\mathrm{d}t}x_{i,j} \\
&+ \beta_i\frac{\partial(K_{i,j})}{\partial x_i}^{\mathrm{T}}\frac{\mathrm{d}x_i}{\mathrm{d}t}x_{i,j} - \frac{\mathrm{d}x_{i,j}}{\mathrm{d}t}\Bigg] = 0
\end{aligned}$$

This allows us to write, for $i \in$ TRAYS:

$$\frac{\mathrm{d}T_i}{\mathrm{d}t} = -\frac{\sum_{j\in\text{COMP}}[(\mathrm{d}\beta_i/\mathrm{d}t)K_{i,j}x_{i,j} + \beta_i(\partial(K_{i,j})/\partial x_i)^{\mathrm{T}}(\mathrm{d}x_i/\mathrm{d}t)x_{i,j} - (\mathrm{d}x_{i,j}/\mathrm{d}t)]}{\sum_{j\in\text{COMP}}\beta_i(\partial(K_{i,j})/\partial T_i)x_{i,j}} \tag{29}$$

where $\partial(K_{i,j})/\partial x_i$ represents the Jacobian of equilibrium ratio $K_{i,j}$ with respect to the liquid mole fractions. We also note that the left hand side of the heat balance can be rewritten as:

$$M_i\frac{\mathrm{d}h_i^l}{\mathrm{d}t} = M_i\left(\frac{\partial h_i^l}{\partial T_i}\frac{\mathrm{d}T_i}{\mathrm{d}t} + \frac{\partial h_i^l}{\partial x_i}^{\mathrm{T}}\frac{\mathrm{d}x_i}{\mathrm{d}t}\right) \tag{30}$$

By introducing dummy variables for $\mathrm{d}T_i/\mathrm{d}t$ and $\mathrm{d}x_{i,j}/\mathrm{d}t$, as in the method of Mattson and Soderlind (1993), we can add the following algebraic equations:

$$\bar{T}_i = -\frac{\sum_{j\in\text{COMP}}[((\mathrm{d}\beta_i/\mathrm{d}t)K_{i,j} + \beta_i(\partial(K_{i,j})/\partial x_i)^{\mathrm{T}}\bar{x}_i)x_{i,j} - \bar{x}_{i,j}]}{\sum_{j\in\text{COMP}}\beta_i(\partial(K_{i,j})/\partial T_i)x_{i,j}} \tag{31}$$

$$\begin{aligned}
M_1\bar{x}_{1,j} &= L_2(x_{2,j} - x_{1,j}) - V_1(y_{1,j} - x_{1,j}) \\
&\quad + F_1(z_{1,j}^f - x_{1,j})
\end{aligned} \tag{32}$$

$$\begin{aligned}
M_i\bar{x}_{i,j} &= V_{i-1}(y_{i-1,j} - x_{i,j}) \\
&\quad + L_{i+1}(x_{i+1,j} - x_{i,j}) - V_i(y_{i,j} - x_{i,j}) \\
&\quad + F_i(z_{i,j}^f - x_{i,j}) \quad i \in \text{TRAYS} \setminus \{1, N\}
\end{aligned} \tag{33}$$

$$\begin{aligned}
M_N\bar{x}_{N,j} &= V_{N-1}(y_{N-1,j} - x_{N,j}) \\
&\quad - V_N(y_{N,j} - x_{N,j}) + F_N(z_{N,j}^f - x_{N,j})
\end{aligned} \tag{34}$$

$$\begin{aligned}
M_1\left(\frac{\partial h_1^l}{\partial T_1}\bar{T}_1 + \frac{\partial h_1^l}{\partial x_1}^{\mathrm{T}}\bar{x}_1\right) &= L_2(h_2^l - h_1^l) - V_1(h_1^v - h_1^l) \\
&\quad + F_1(h_1^f - h_1^l) + Q_r
\end{aligned} \tag{35}$$

$$\begin{aligned}
&M_i\left(\frac{\partial h_i^l}{\partial T_i}\bar{T}_i + \frac{\partial h_i^l}{\partial x_i}^{\mathrm{T}}\bar{x}_i\right) \\
&= V_{i-1}(h_{i-1}^v - h_i^l) + L_{i+1}(h_{i+1}^l - h_i^l) - V_i(h_i^v - h_i^l) \\
&\quad + F_i(h_i^f - h_i^l) \quad i \in \text{TRAYS} \setminus \{1, N\}
\end{aligned} \tag{36}$$

$$\begin{aligned}
&M_N\left(\frac{\partial h_N^l}{\partial T_N}\bar{T}_N + \frac{\partial h_N^l}{\partial x_N}^{\mathrm{T}}\bar{x}_N\right) \\
&= V_{N-1}(h_{N-1}^v - h_N^l) - V_N(h_N^v - h_N^l) \\
&\quad + F_N(h_N^f - h_N^l) - Q_c
\end{aligned} \tag{37}$$

and also drop the heat Eq. (28). Note that these last algebraic equations are explicit in V_i and this leads to an index one system. This approach was used in (Biegler, Cervantes, & Wächter, 2002; Cervantes et al., 2000). However, in our complementarity formulation we note that there is no relation that defines $\mathrm{d}\beta_i/\mathrm{d}t$. To deal with this term we consider three cases:

- When two phases are present, $\beta = 1$, $\mathrm{d}\beta/\mathrm{d}t = 0$ and therefore $\sum_{j\in\text{COMP}}(\mathrm{d}\beta_i/\mathrm{d}t)K_{i,j}x_{i,j} = 0$.
- When only the vapor phase is present, we have $\beta \leq 1$ and from complementarity, $M_i = M_i^l = 0$ for $i = 1, \ldots, N$. As a result, the left hand sides of the heat and mass balance equations disappear and the values of $\mathrm{d}\beta/\mathrm{d}t$ and $\bar{x}_i$ are unimportant.
- On the other hand, when only the liquid phase is present, we have $\beta \geq 1$. For this, one needs to derive additional expressions for $\mathrm{d}\beta/\mathrm{d}t$ using the complementarity equa-

tions. Because of the ill-conditioned limiting behavior of these equations, we believe that this represents an unnecessarily difficult case. Instead, the index one formulation in Section 3 should be considered for this case.

As a result of these arguments, we consider only transitions from all vapor to two phase (and vice versa) with this simplified model.

The results we present in the next two sections are from optimization of the start-up of the columns described above. The results are quite interesting in that the presence and absence of phases can be captured naturally using a single set of equations in a dynamic setting.

5. Example problem: batch distillation

We first consider a batch distillation column with $F_i(t) = 0, i \in \text{TRAYS}$. The batch column is charged with feed consisting of a mixture of benzene and toluene in the bottom tray, $i = 1$. The mole fraction of the benzene in the feed is 0.58 and the column is operated at a pressure of 100 kPa. The column consists of $N = 12$ trays (including the reboiler and condenser). The initial charge to the column is $M_1(0) = 8$ kmol and the maximum reboiler heat duty is set to 600 kJ/h. The minimum holdup required for liquid flow from a tray are chosen as,

$$M_{\min,i} = \begin{cases} 0.3 & i \in \text{TRAYS} \setminus \{N\} \\ 0.5 & i = N. \end{cases}$$

The column is fitted with a complete condenser. As a result, $V_N = 0$ and the (bubble point) phase equilibrium relations in (22) for the condenser ($i = N$) can be posed as,

$$\begin{aligned} y_{N,j} &= K_{N,j}(T_N, P_N, x_N)x_{N,j} \quad j \in \text{COMP} \\ 0 &= \sum_{j\in\text{COMP}} y_{N,j} - \sum_{j\in\text{COMP}} x_{N,j}. \end{aligned} \tag{38}$$

Similarly, the equation for $\bar{T}_N$ in (31) can be simplified for $i = N$ as,

$$\bar{T}_N = -\frac{\sum_{j\in\text{COMP}}[((\partial(K_{N,j})/\partial x_N)^{\mathrm{T}}\bar{x}_N)x_{N,j} - \bar{x}_{N,j}]}{\sum_{j\in\text{COMP}}(\partial(K_{N,j})/\partial T_N)x_{N,j}}. \tag{39}$$

At initial time, the holdup on the trays, $i \in \text{TRAYS} \setminus \{1\}$ in the column are set to zero and the composition of the liquid on the trays is set to that of the feed. In other words,

$$\begin{aligned} M_i^l(0) &= \begin{cases} 8 \text{ if } i = 1 \\ 0 \text{ if } i \in \text{TRAYS} \setminus \{1\} \end{cases} \\ x_i(0) &= [0.58, 0.42]^{\mathrm{T}} \quad i \in \text{TRAYS} \end{aligned} \tag{40}$$

The control variables in the column operation are the distillate withdrawal, D and the reboiler heat duty, Q_r. The start-up of the column is posed as a free end-time problem which maximizes the average rate of product withdrawal over the time of operation t_f as follows,

$$\begin{aligned} \max \quad & \frac{1}{t_f}\left(\int_0^{t_f} D(t)dt + M_N^l(t_f)\right) \\ & -\epsilon\frac{1}{t_f}\int_0^{t_f}(Q_r(t) - Q_r^{\max})^2 \mathrm{d}t \\ \text{s.t.} \quad & \text{Eqs. (19), (25)(27), (31)(37), (40)} \\ & \frac{\int_0^{t_f} D(t)x_{N,\text{benzene}}(t)\mathrm{d}t + M_N^l(t_f)x_{N,\text{benzene}}(t_f)}{\int_0^{t_f} D(t)\mathrm{d}t + M_N^l(t_f)} \\ & \geq 0.95. \end{aligned} \tag{41}$$

where $\epsilon > 0$ is a small parameter serving to regularize the singular control problem. The first term in the objective function is clearly bounded above since the amount of initial feed to the batch column is fixed. On the other hand, the second term is bounded above by zero and attempts to find controls, $Q_r(t)$ that are "close" to $Q_r^{\max}$ for all time t. In the above formulation, the total product at final time is defined as the sum of the condenser holdup at final time and the total distillate withdrawal over time. The total product that is withdrawn from the column is required to have a certain purity of benzene as indicated by the last constraint of the optimization problem (41). A lower bound of 10 kJ/h is placed on the reboiler heat duty, Q_r to prevent the vapor flowrate from vanishing.

The optimal control problem is discretized over 30 elements with 2 collocation points leading to a problem with 22226 variables and 20125 constraints including 2040 complementarity constraints. The problem solved to a tolerance of 10^{-5} in the optimality conditions using a 2.2 GHz Intel Pentium IV processor running LINUX as the operating system. IPOPT-C required 153 iterations and 3.1 CPU hours to obtain the solution.

The optimization yields the time for operation as 28.8 h. The profiles of liquid holdup, liquid flows and vapor flows in the optimal solution are shown in Figs. 1, 3 and 4 respectively. The trays have no liquid holdup at initial time (40), hence no liquid flows from the trays until the liquid holdup

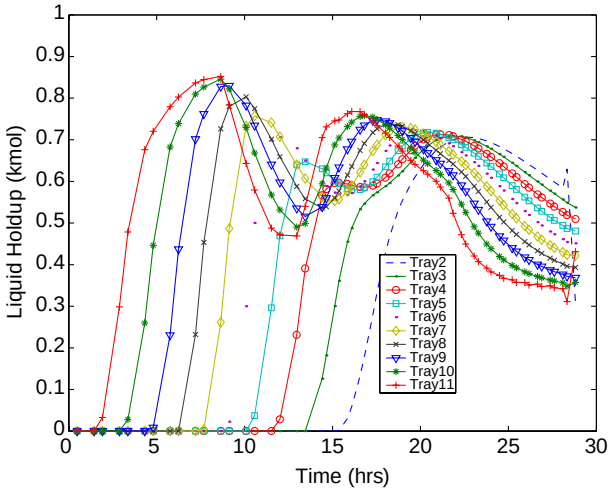

Fig. 1. Liquid holdup profile on trays, $i \in \text{TRAYS}\setminus\{1, N\}$ in batch column.

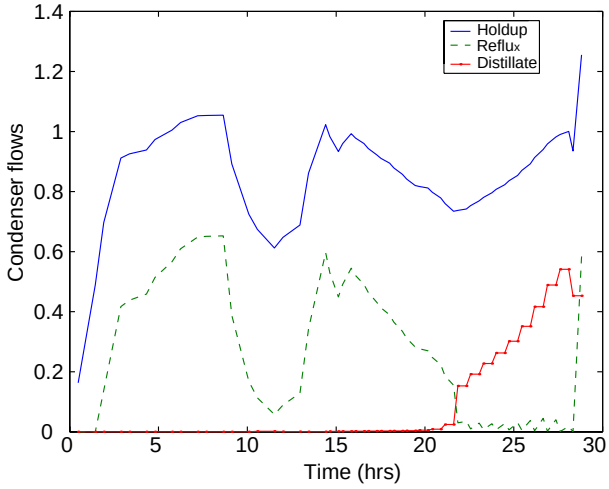

Fig. 2. Liquid holdup and flow from the condenser in the batch column.

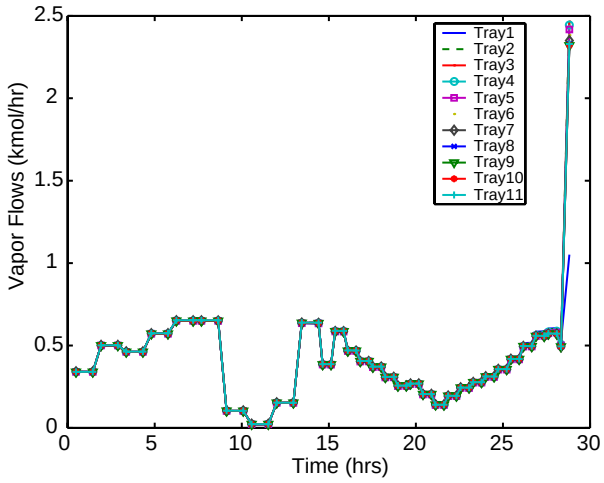

Fig. 4. Vapor flow in the batch column.

(see Fig. 3) is at least equal to the minimum threshold (see Fig. 1). Since the model assumes no vapor holdup the vapor flow is the same throughout the column, see Fig. 4. The vapor from the bottom is completely condensed on tray N and refluxed to the column at initial time. This helps to increase the holdup on the trays. The holdups on the trays increase in the decreasing order of tray number (see Fig. 1 and 2). The overall fluctuations in the liquid holdup correspond to the fluctuations in vapor flowrate (see Figs. 3 and 4).

Note that the trends in vapor flowrate correspond to that of the reboiler heat duty, Q_r. The optimal profile of heat duty is shown in Fig. 5. The profile of benzene compositions in the holdups on trays are provided in Fig. 6. When no tray holdup is present, the liquid composition on trays is similar to the bottom composition. This is also true of the vapor composition on trays without holdup and hence, the attainment of equilibrium on all trays is instantaneous. The benzene composition in the condenser initially increases and subsequently, takes a downturn as the bottom becomes leaner

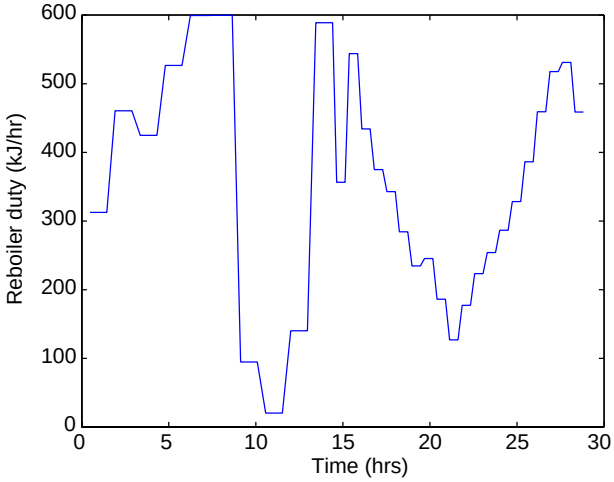

Fig. 5. Optimal reboiler heat duty profile in the batch column.

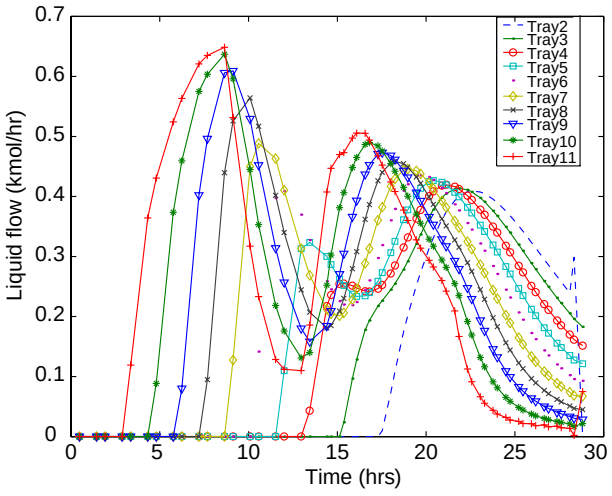

Fig. 3. Liquid flow from trays, $i \in \text{TRAYS} \setminus \{1, N\}$ in the batch column.

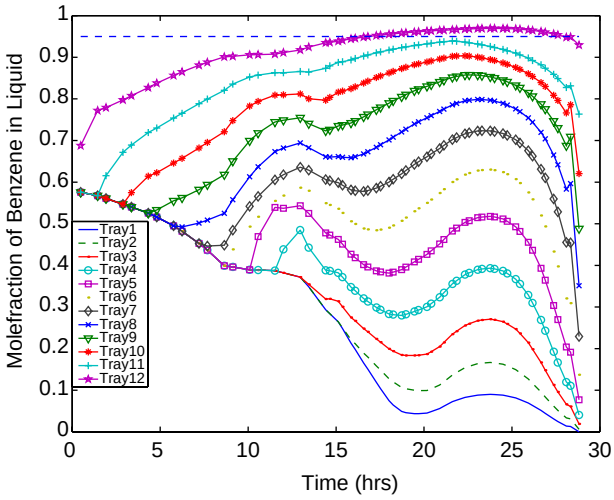

Fig. 6. Composition profile of benzene in liquid holdup on trays in the batch column.

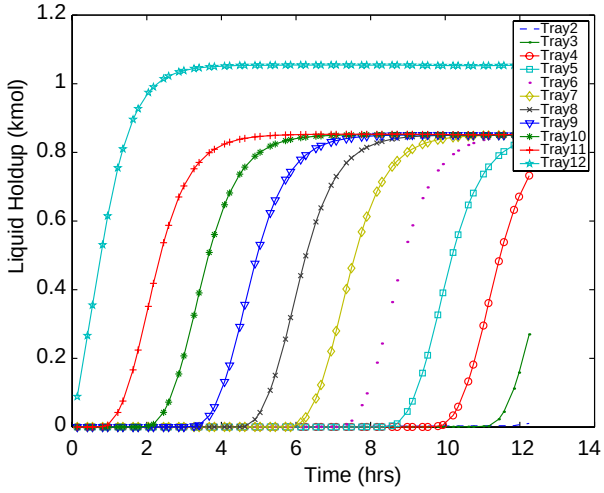

Fig. 7. Liquid holdup on the trays when $Q_r = 600$ kJ/h in the batch column.

in benzene. At final time, the composition of benzene in the condenser holdup is lower than the required 0.95 mole fraction of benzene. However, the distillate withdrawn has a much higher benzene composition, so that the required purity constraint is exactly satisfied at the solution.

The optimal reboiler heat duty profile seems to counter intuition. The intuitive notion might be to operate at maximum reboiler heat duty and withdraw distillate only when the required purity is reached. Unfortunately, such a policy will not be successful. Either no holdup appears on some trays or the condenser composition at final time will be less than 0.95 in benzene. Fig. 7 shows that tray 2 has no holdup when all of the initial charge in the bottoms has vaporized. The composition of benzene in the condenser (see Fig. 8) is lower than 0.95 at this time. In addition, the trays 1, 2 and 3 are much leaner in benzene. This implies that we will have to shut down the reboiler heat duty and opt for building more product in the bottoms using the liquid overflow from the trays above. The maximum boilup policy possesses some drawbacks,

- the case of no vapor flowrate cannot be handled by the model
- mole fraction of benzene in the bottoms charge will be much lower.

This indicates that a maximum reboiler heat duty operating policy is undesirable.

In fact, the counter intuitive optimal reboiler heat duty profile indicates an over-capacity due to a poor design. A reduction in the maximum reboiler heat duty to $Q_r^{\max} = 300$ kJ/h and a reduction in the tray hold-ups ($M_{\min,N} = 0.3$, $M_{\min,i} = 0.1$ otherwise) does lead to the intuitive operating policy, with the heat duty at the upper bound, as the optimal policy.

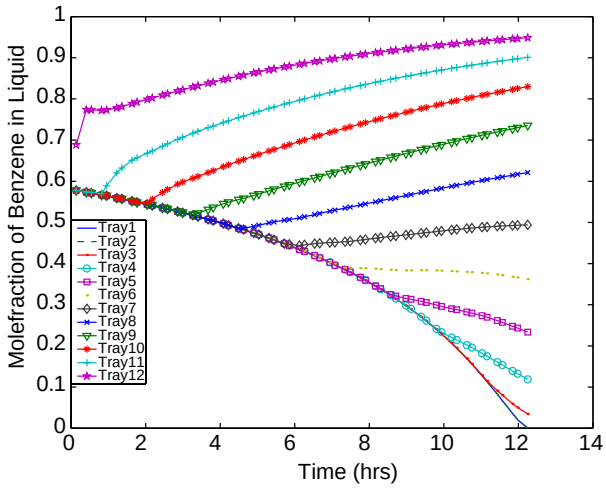

Fig. 8. Composition profile of benzene in liquid holdup on trays in the batch column when $Q_r = 600$ kJ/h.

6. Case study: switching operating modes in cryogenic plants

This section addresses dynamic optimization of a large-scale natural gas processing plant through the formulation of detailed dynamic models. In previous work (Diaz, Tonelli, Bandoni, & Biegler, 2003), a dynamic optimization problem was formulated and solved using SRK thermodynamics and CO_2 solubility predictions. However, two phases were assumed at all times on the trays. Our study generalizes this work to deal with changes in the number of phases during startup and transition of operating conditions.

Natural Gas Liquids (NGL) are light hydrocarbons in the range of ethane through hexane plus, which may be recovered as liquids from a natural gas source. NGL processing plants provide feed-stock, mainly ethane and propane, for production of olefins and other petrochemicals. Turboexpansion processes are currently the most efficient ones for obtaining high ethane recovery. The separation is performed at high pressure and cryogenic conditions. Wilkinson and Hudson (1982) have proposed different turboexpansion plant designs to improve ethane recovery. Diaz, Serrani, Bandoni, and Brignole (1997) have solved the debottlenecking problem of an ethane extraction plant as a Mixed Integer Nonlinear Programming (MINLP) model. Dynamic simulation of complex cryogenic processes has been studied by a few authors. Mandler (2000) has studied dynamic simulation of liquefied natural gas plants and air separation plants for control analysis and design in liquefaction processes. However, dynamic optimization of entire plants has not been addressed until the last decade. This work addresses the dynamic optimization of a part of the cryogenic section in a natural gas processing plant. The demethanizing column, together with the turboexpander, constitutes the main part of the cryogenic separation. The model comprises differential energy and mass balances, hydraulic correlations and ideal thermodynamic predictions. In this section, inlet gas is cooled by

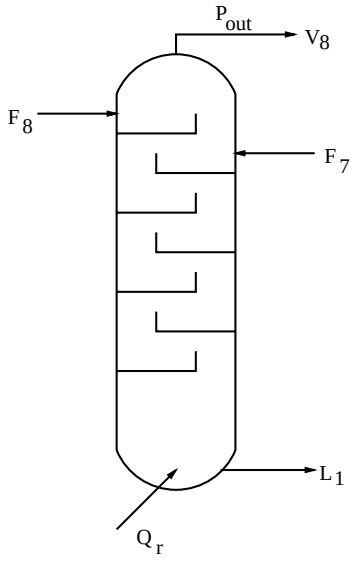

Fig. 9. Schematic of a cryogenic distillation column.

heat exchange with residual gas and demethanizer side and bottom reboilers. The partially condensed gas feed is then sent to a high-pressure separator. The vapor is expanded through a turboexpander to obtain the low temperatures required for high ethane recovery and is then fed to the top of the demethanizer column. The liquid from the high pressure separator enters the demethanizer at its lowest feed point. Methane and lighter components constitute the top product and ethane and heavier hydrocarbons are obtained as bottoms product. Carbon dioxide is distributed between top and bottom streams.

The cryogenic column is used for the stripping of a mixture consisting of *nitrogen*, *methane*, *ethane*, *propane*, *carbon-dioxide*, *n-butane*, *iso-butane*, *n-pentane*, *iso-pentane* and *hexane*. A schematic of the cryogenic distillation column is provided in Fig. 9. The column has $N = 8$ trays and is also started with no initial component holdup on the trays and a charge on the bottom tray alone. The charge in the bottom consists predominantly of liquid in equilibrium with its vapors. The dynamics differ substantially from the previous column due to modeling of the vapor holdup and variable pressure on trays. The total volume on each tray is assumed to consist of volumes of the liquid and vapor holdups (refer (24)). However, if no initial component holdup is assumed, then the equation defining liquid and vapor densities (24) cannot be satisfied. To circumvent this, we have assumed that all the trays except the bottom have vapor holdup consisting of an inert component alone, as suggested by Marquardt (personal communication). The equilibrium constant for the inert ($K_{i,\text{inert}}$) is taken to be a large quantity indicating that it is not condensible, accumulating preferentially in the vapor phase.

The control variables in the column are the top withdrawal pressure (P_{out}) and the bottom reboiler heat duty (Q_r). For this case the feeds F_7 and F_8 are specified, $F_i = 0, i \in \text{TRAYS} \setminus \{7, 8\}$ and $Q_c = 0$. Due to the increased number of components the discretized problem scales up faster than the previous model. Further, the stiff dynamics resulting from the modeling of the vapor flows need to be resolved using a fine mesh. With this in mind, we have split the short term start-up operation into the following three time periods.

1. The first period aims to form liquid on all but the feed trays ($i = \{7, 8\}$) by evaporating the bottoms charge. There is no feed to the column and no product withdrawal from the bottoms. The withdrawal side pressure is maintained constant at $P_{\text{out}} = 18$ bar and hence, the liquid build-up needs to be achieved using the reboiler heat duty as a control variable. The amount of liquid holdup required is very small but sufficient to ensure equilibrium on all the trays as modeled by the equations in (22). The objective is to minimize time needed to accomplish this.
2. Next we increase the holdup levels so that we have liquid flowing from all the trays. For this we supply feed on both trays, $i = \{7, 8\}$ with molar flowrates of $F_7 = 30$ and $F_8 = 100$ kmol/min. For this operation we use both withdrawal pressure and reboiler heat duty as control variables. We aim to minimize the operation time through minimal use of reboiler heat duty.
3. Finally, we aim to achieve a steady state where we can recover most of the ethane in the feeds as the bottoms product. The optimal control is performed over a fixed time horizon of $t_f = 10$ min for this stage.

The optimization problem for the three periods are given in Table 1. These also include the Eqs. (19)–(26) in addition to the constraints in Table 1. The problems are discretized over 12 finite elements with 2 collocation points to yield a NLP. Information on problem size on discretization and computational requirements for the solution of the three cases is provided in Table 2. All problems have been solved to a tolerance of 10^{-4} in the optimality conditions. Observe

Table 1
Optimization formulation for different periods

	Period 1	Period 2	Period 3
Objective	$\min t_f$	$\min t_f + 0.1 \int_0^{t_f} Q_r(t)\mathrm{d}t$	$\min \int_0^{t_f} \left(\frac{L_1(t)x_{1,\text{C2}}}{F_7 z^f_{7,\text{C2}} + F_8 z^f_{8,\text{C2}}} - 1 \right)^2 \mathrm{d}t$
Controls	Q_r	P_{out}, Q_r	P_{out}, Q_r
Feed	$F_7 = 0$, $F_8 = 0$	$F_7 = 30$, $F_8 = 100$	$F_7 = 60$, $F_8 = 250$
Final time constraint	$M^l_6(t_f) \geq 10^{-4}$	$L_2(t_f) \geq 1$	$x_{1,\text{C2}}(t_f) \geq 0.5$

Table 2
Problem characteristics and computational requirements for IPOPT-C on the cryogenic distillation case study

	Period 1	Period 2	Period 3
# variables	17918	17942	17944
# constraints	17318	17330	17344
# complementarity cons.	575	575	576
# iterations	624	104	97
# CPU time (h)	30	3.8	8.4

The results are obtained on a 2.2 GHz Intel Xeon processor running LINUX as the operating system.

that the solution for Period 1 requires more iterations for its solution and amply reflects the nature of the problem that is solved. One cause for the difficulty in solving the Period 1 problem is that most of the compositions (except for inert) are zero. This results in poor conditioning of the matrix (also called the KKT matrix) in the linear system that calculates the search direction. Nevertheless, by inertia corrections in IPOPT, a nonsingular system is solved to obtain a stable solution. The computationally intensive step in each iteration is the factorization of the KKT matrix to obtain a search direction. The KKT matrix requires modification and re-factorization if some heuristics on the inertia of the linear system (Wächter, 2002; Wächter & Biegler, 2004) are not satisfied. This leads to the large computational time per iteration. This is also the cause for Period 3 requiring more time per iteration as compared to Period 2.

We first present results for Period 1. The minimum time is achieved by supplying the maximum reboiler duty to the bottom which is 550 MJ/min. The formation of liquid occurs by a different process as compared to the previous column. Liquid is formed on a tray when the higher temperature vapors from the bottom contact with the cold inert vapor on the trays above. Hence, the formation of liquid (see Fig. 10) and achievement of equilibrium on trays (see Fig. 11) occur sequentially starting from the lower numbered trays. Further, the inert composition on each tray decreases with time, refer Fig. 12.

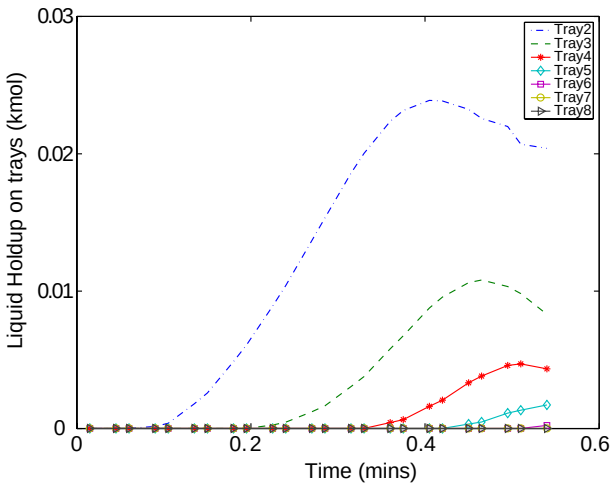

Fig. 10. Liquid holdup profiles in Period 1 solution.

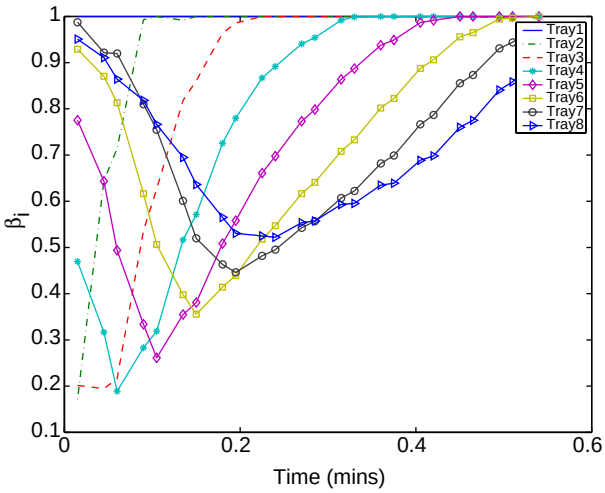

Fig. 11. Equilibrium indicator (β_i) profiles in Period 1 solution.

In the second period, we minimize the operation time by using the reboiler heat duty and withdrawal side pressure profiles as depicted in Figs. 13 and 14, respectively. The feed to the top trays of the column and changing withdrawal pressure play the pivotal role in ensuring liquid holdup on all trays (see Fig. 15). In contrast to Period 1, the holdup now increases in decreasing order of tray number. The liquid flow from the trays corresponds to the liquid holdup as observed from Fig. 16. The feed F_7 is just liquid while F_8 consists predominantly of vapor. As a result, tray 7 builds up faster than tray 8 and also has a higher liquid flowrate as can be seen from Figs. 15 and 16. The composition of inert in the vapor on trays further decreases to negligible levels, refer Fig. 17.

Finally, the third period brings the column to steady state operation. The objective in the third period reflects the recovery of ethane in the feed that is required in the bottom products. The optimal control problem also includes a final time constraint on the mole fraction of ethane in the bot-

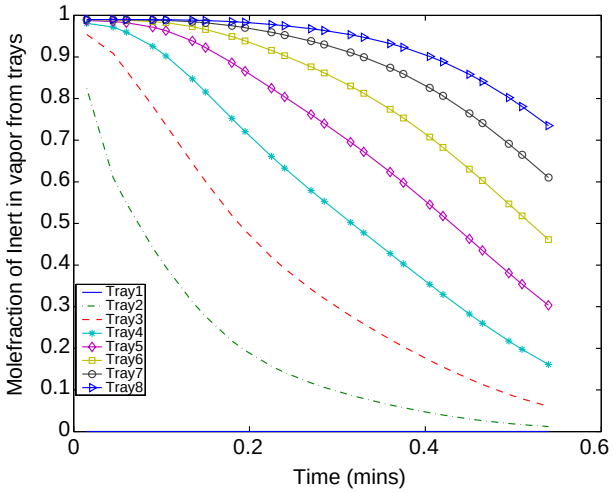

Fig. 12. Inert composition profiles in Period 1 solution.

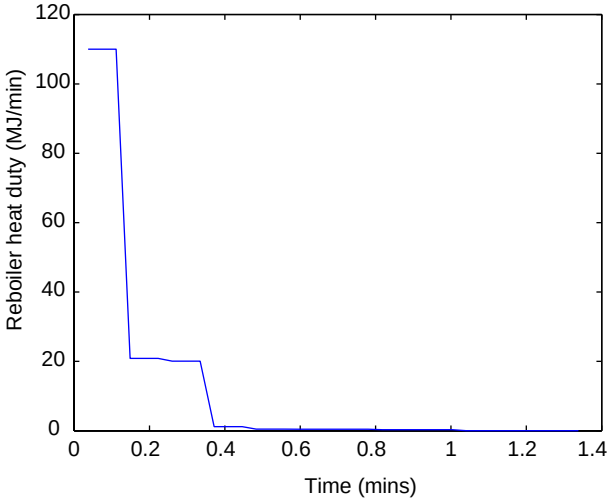

Fig. 13. Reboiler heat duty (Q_r) profile in Period 2 solution.

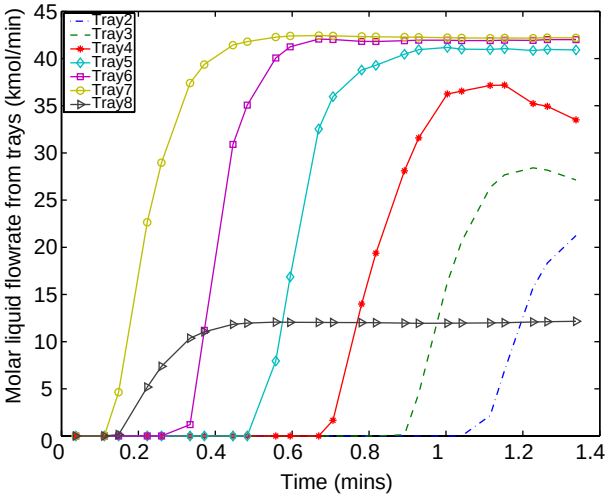

Fig. 16. Liquid flow (L_i) profiles in Period 2 solution.

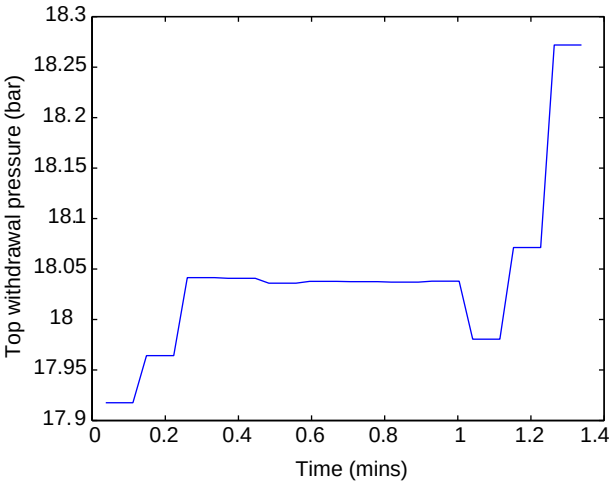

Fig. 14. Withdrawal side pressure (P_{out}) profile in Period 2 solution.

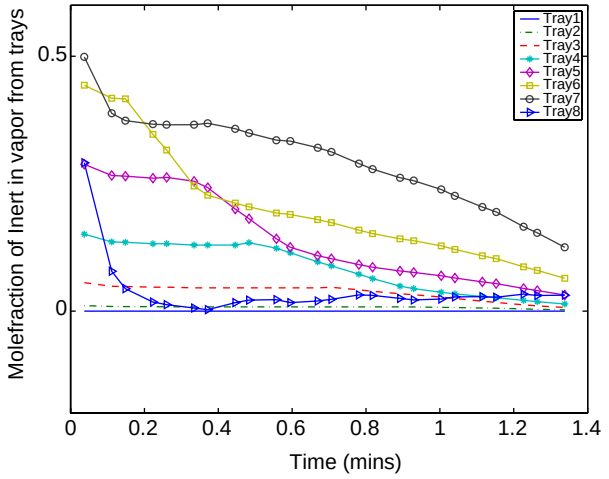

Fig. 17. Profiles of inert composition in vapors ($y_{i,\text{inert}}$) in Period 2 solution.

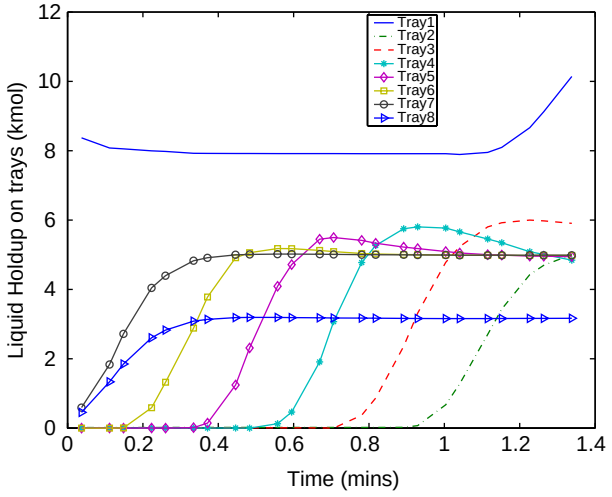

Fig. 15. Liquid holdup (M_i^l) profiles in Period 2 solution.

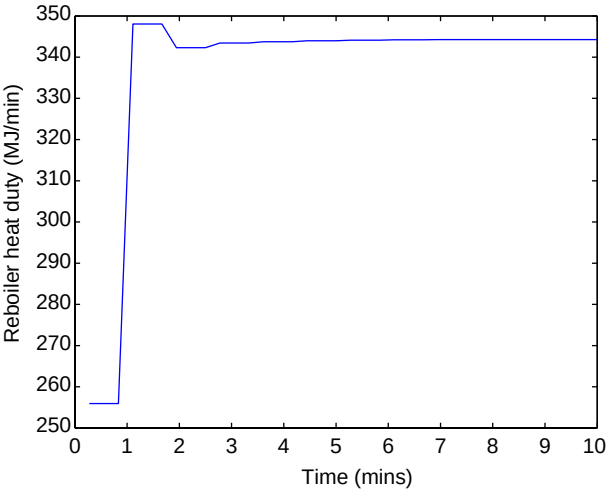

Fig. 18. Reboiler heat duty (Q_r) profile in Period 3 solution.

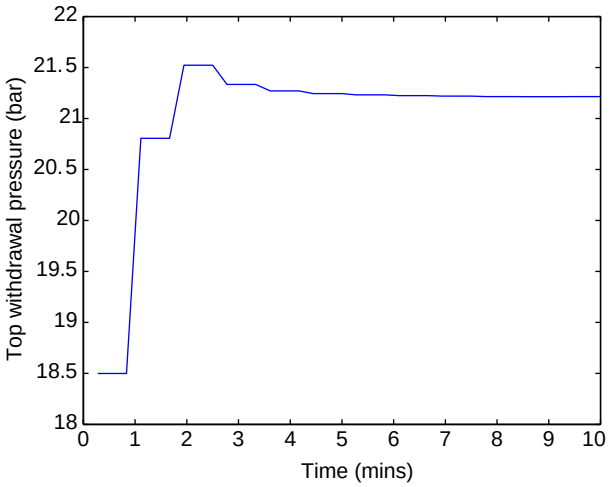

Fig. 19. Top withdrawal pressure (P_{out}) profile in Period 3 solution.

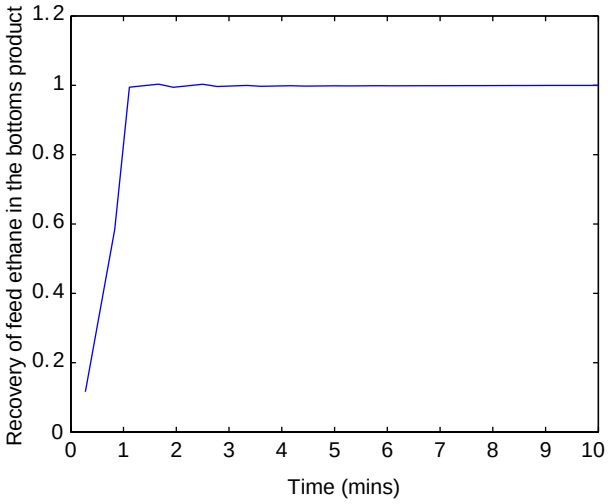

Fig. 20. Profile of feed ethane recovery in the bottoms product of Period 3 solution.

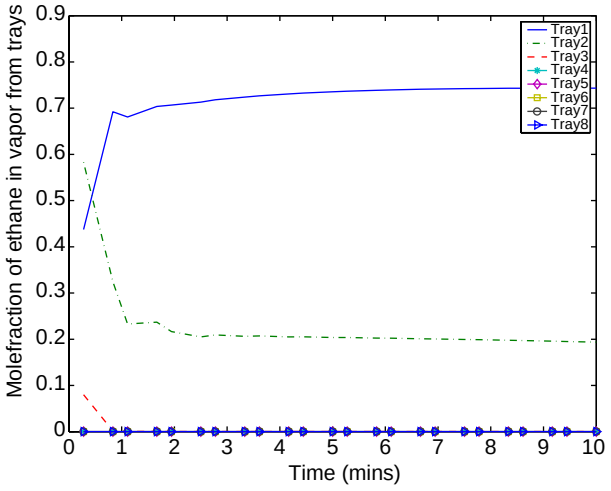

Fig. 21. Profile of ethane composition in vapors from the trays of column in Period 3 solution.

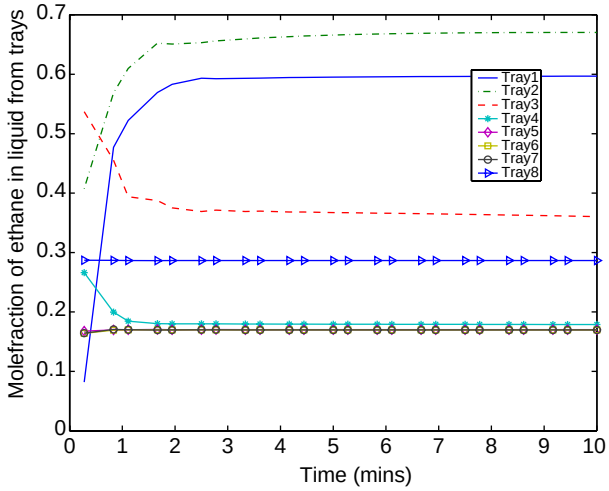

Fig. 22. Profile of ethane composition in liquid from the trays of column in Period 3 solution.

toms product. The feed flowrates for this period are nearly 2.5 times that in the second period. The optimal profiles of the reboiler heat duty, Q_r and the withdrawal pressure, P_{out} are provided in Figs. 18 and 19 respectively. The optimal recovery of feed ethane in the bottoms product is presented in Fig. 20. The recovery of ethane in the bottoms product increases steadily towards 1. It is clear that in the final solution all of the feed ethane is in the bottoms product. Hence, the mole fraction of ethane in the vapors exiting from the column is negligible (refer Fig. 21) while the composition of ethane in the bottoms product is much greater than the requirement at final time (refer Fig. 22).

7. Conclusions

With growing interest in dynamic optimization in process engineering, hybrid systems and discrete events are also starting to be considered. This study explores the use of complementarity formulations to deal with one class of dynamic hybrid systems: phase transitions in the dynamic operation of distillation columns. Here we introduce complementarity relations through a simple modification of the tray equilibrium equations. The resulting mathematical program with equilibrium constraints (MPEC) is a single, large-scale, continuous variable formulation. While the MPEC formulation does not satisfy nonlinear programming constraint qualifications, we show how it can be solved by using IPOPT-C, an extension of the large-scale NLP algorithm IPOPT.

This study considers both index one and index two formulations for the dynamic distillation models (with and without vapor holdup on trays, respectively). Our first application uses the simpler model (without vapor holdup) to deal with the optimal (cold) startup of a binary batch distillation column, initially with no liquid on the trays. In the second study, we consider the more detailed model for the startup of a cryogenic multicomponent separation of natural gas liq-

uids. Enabled by the complementarity formulations and the IPOPT-C solver, this approach allows us to model the appearance and disappearance of phases during the dynamic optimization. This approach leads to very interesting and often counter-intuitive solution profiles.

The results presented here are some of the first for the optimization of hybrid dynamical systems modeled through a complementarity formulation. This study raises interesting questions on the applicability of the complementarity formulation to other classes of hybrid systems. It is imperative to identify the classes of discontinuous systems that can be modeled effectively using a complementarity formulation. Issues of stability and convergence of the discretization are also important.

In future work, we intend to explore several issues that will improve the performance of the IPOPT-C solver. These include improved linear factorizations, parallel decomposition strategies for the discretized dynamic equations and refinement of IPOPT-C algorithm. Additionally, better handling of negative curvature is required to avoid excessive linear factorizations on large systems. These developments will also be augmented through the integration of process modeling tools, graphical interfaces and nonlinear solvers. Finally, we intend to consider a wider class of hybrid system applications, including the incorporation of stability and controllability constraints within the DAE model.

Acknowledgements

The authors thank Prof. W. Marquardt for interesting discussions on dynamic distillation models. Funding for this work was provided through a Fulbright Fellowship for M.S. Diaz, through the National Science Foundation (CTS-0314647) and through a Honeywell subcontract from the Defense Advanced Research Projects Agency.

References

Allgor, R., & Barton, P. I. (1999). Mixed integer dynamic optimization i: problem formulation. *Computers and Chemical Engineering, 23*(4/5), 457.

Anitescu, M. (2001). *On solving mathematical programs with complementarity constraints as nonlinear programs*. Technical report ANL/MCS-P864-1200. Mathematics and Computer Science Division, Argonne National Laboratory, Argonne, IL.

Avraam, M., Shah, N., & Pantelides, C. C. (1998). Modeling and optimization of general hybrid systems in continuous time domain. *Computers and Chemical Engineering, 22*, S221.

Bader, G., & Ascher, U. (1987). A new basis implementation for mixed order boundary value ode solver. *SIAM Journal on Scientific and Statistical Computing, 8*, 483–500.

Barton, P. I., Allgor, R. J., Feehery, W. F., & Galan, S. (1998). Dynamic optimization in a discontinuous world. *Industrial & Engineering Chemistry Research, 37*, 966–981.

Barton, P. I., & Park, T. (1997). Analysis and control of combined discrete/continuous systems: Progress and challenges in the chemical process industries. *AIChE Symposium Series, 93*(316), 102.

Biegler, L. T., Cervantes, A. M., & Wächter, A. (2002). Advances in simultaneous strategies for dynamic process optimization. *Chemical Engineering Science, 57*, 575.

Cervantes, A. M., & Biegler, L. T. (1998). Large-scale DAE optimization using a simultaneous NLP formulation. *AIChE Journal, 44*(5), 1038.

Cervantes, A. M., Wächter, A., Tütüncü, R., & Biegler, L. T. (2000). A reduced space interior point strategy for optimization of differential algebraic systems. *Computers and Chemical Engineering, 24*, 39–51.

Clark, P. A., & Westerberg, A. W. (1990). Bilevel programming for steady state chemical process design i. *Computers and Chemical Engineering, 14*(1), 87–97.

Diaz, S., Serrani, A., Bandoni, A., & Brignole, E. (1997). Automatic design and optimization of natural gas plants. *Industrial & Engineering Chemistry Research, 36*, 715–724.

Diaz, S., Tonelli, S., Bandoni, A., & Biegler, L. T. (2003). Dynamic optimization for switching between operating modes in cryogenic plants. In Proceedings of FOCAPO 2003, Coral Springs, Miami, USA, (p. 601).

Fiacco, A. V., & McCormick, G. P. (1968). *Nonlinear programming: sequential unconstrained minimization techniques*. Reprinted by SIAM Publications. New York, USA: Wiley.

Fletcher, R., Gould, N. I. M., Leyffer, S., Toint, Ph. L., & Wächter, A. W. (1999). *Global convergence of trust-region sQP-filter algorithms for nonlinear programming*. Technical report 99/03, Department of Mathematics, University of Namur, Namur, Belgium.

Fletcher, R., Leyffer, S., Ralph, D., & Scholtes, S. (2002). *Local convergence of SQP methods for mathematical programs with equilibrium constraints*. Technical report NA\209, University of Dundee, UK.

Floudas, C. A., & Grossmann, I. E. (1987). Synthesis of flexible heat exchanger networks with uncertain flowrates and temperatures. *Computers and Chemical Engineering, 11*, 319–336.

Forsgren, A., Gill, P. E., & Wright, M. H. (2002). Interior methods for nonlinear optimization. *SIAM Review, 44*(4), 525–597.

Fourer, R., Gay, D., & Kernighan, R. (2001). AMPL. Cole/Brooks.

Gill, P. E., Murray, W., & Saunders, M. A. (2002). SNOPT: An SQP algorithm for large-scale constrained optimization. *SIAM Journal on Optimization, 12*(4), 979–1006.

Gopal, V., & Biegler, L. T. (1999). Smoothing methods for Complementarity Problems in Process Engineering. *AIChE Journal, 45*(7), 1535–1547.

Harker, P. T., & Pang, J.-S. (1990). Finite-dimensional variational inequalities and complementarity problems: a survey of theory, algorithms and applications. *Mathematical Programming, 60*, 161–220.

Heemels, W. P., DeSchutter, B., & Bemporad, A. (2001). On the equivalence of hybrid dynamical models. In 40th IEEE Conference on Decision and Control, Orlando, FL, (pp. 364–369).

Lang, Y. -D., & Biegler, L. T. (2002). A distributed stream method for tray optimization. *AIChE Journal, 48*(3), 582.

Leyffer, S., & Fletcher, R. (2000). Mathematical programs with equilibrium constraints. In International Symposium on Mathematical Programming, Atlanta, GA.

Luo, Z. -Q., Pang, J. -S., & Ralph, D. (1996). *Mathematical programs with equilibrium constraints*. Cambridge: Cambridge University Press.

Mandler, J. A. (2000). Modelling for control analysis and design in complex industrial separation and liquefaction processes. *Journal of Process Control, 10*(2), 167–175.

Mattson, S., & Soderlind, G. (1993). Index reduction in differential algebraic systems using dummy derivatives. *SIAM Journal on Scientific Computing, 14*, 677–692.

Pedersen, K. S., Fredenslund, Aa., & Thomassen, P. (1989). *Properties of oils and natural gases*. Gulf Publishing Company, Houston.

Raghunathan, A. U., & Biegler, L. T. (2004). Interior point methods for mathematical programs with complementarity constraints (MPCCs). *SIAM J. Optimization*, to appear.

Raghunathan, A. U., & Biegler, L. T. (2003). MPEC formulations and algorithms in process engineering. *Computers and Chemical Engineering*, *27*, 1381–1392.

Raghunathan, A. U., Perez-Correa, R., & Biegler, L. T. (2003). Data reconciliation and parameter estimation in flux-balance analysis. *Biotechnology and Bioengineering*, *84*, 700–709.

Sahin, K. H., & Ciric, A. R. (1998). A dual temperature simulated annealing approach for solving bilevel programming problems. *Computers and Chemical Engineering*, *23*, 11–25.

Stein, O., Oldenburg, J., & Marquardt, W. (2004). Continuous reformulations of discrete-continuous optimization problems. *Computers and Chemical Engineering*, in press.

van der Schaft, A. J., & Schumacher, J. M. (1998). Complemetarity modeling of hybrid systems. *IEEE Transactions on Automatic Control*, *43*(4).

Wächter, A. (2002). *Interior point methods for large-scale nonlinear programming with applications*. Ph.D. thesis, Carnegie Mellon University.

Wächter, A., & Biegler, L. T. (2004). Line search filter methods for nonlinear programming: Motivation and global convergence. *SIAM J. Opt.*, to appear.

Wilkinson, J., & Hudson, H. (1982). Turboexpander plant designs can provide high ethane recoveries without inlet CO_2 removal. *Oil & Gas Journal*, *80*(18), 281.